

## Drop formation in aqueous two-phase systems

R.S. Barhate, Ganapathi Patil, N.D. Srinivas<sup>1</sup>, K.S.M.S. Raghavarao\*

*Department of Food Engineering, Central Food Technological Research Institute, Mysore 570 013, India*

Received 19 June 2003; received in revised form 16 September 2003; accepted 9 October 2003

### Abstract

Extraction using aqueous two-phase systems (ATPSs) is a versatile technique for the downstream processing of various proteins/enzymes. The study of drop formation deals with the fundamental understanding of the behavior of liquid drops under the influence of various external body as well as surface forces. These studies provide a basis for designing of the extractions in column contactors in which liquid drops play a major role. Most of the drop formation studies reported so far is restricted to aqueous–organic systems. ATPSs, differ from aqueous–organic systems in their physical properties. In view of this, an attempt was made to develop a model for drop formation in ATPSs adopting the information available on aqueous–organic systems. In order to validate the model, experiments were performed by using polyethylene glycol (PEG)/salt systems of different phase compositions at various flow rates. At low flow rates the single stage model and at high flow rates the two stage model are able to predict the drop volume during its formation from tip of capillary. The experimental results were found to agree reasonably well with those predicted by the model.

© 2003 Elsevier B.V. All rights reserved.

*Keywords:* Aqueous two-phase system; Drop formation

### 1. Introduction

Extraction using aqueous two-phase systems (ATPSs) is a versatile technique for the downstream processing of various proteins/enzymes. Applications of ATPSs were extensively reviewed [1–5]. When the equilibrated dispersion is separated back into two individual phases, the desired protein concentrates in one of the phases, facilitating its isolation. In some instances one such batch extraction is sufficient to achieve satisfactory separation, while in others, multistage procedure is necessary. For multistage extraction procedures spray columns can be conveniently employed. Further, spray columns enable separation of the phases by gravity easily, eliminating the need for an expensive centrifuge. In addition, they can be adopted easily for continuous processes [6,7].

The study of drop formation deals with the fundamental understanding of the behavior of liquid drops under the influence of various external body as well as surface forces.

These studies provide a basis for understanding of mass transfer during extractions, in which liquid drops play a major role. In case of a spray column, the area available for mass transfer is directly proportional to the average surface area of the individual drops, which in turn, is a function of the volume and shape of the drops.

The models reported in the literature for the predictions of drop volume are pertaining to aqueous–organic systems [8–13]. ATPSs differ from aqueous–organic systems in their physical properties. That is, they have low density and high viscosity differences between the individual phases and low interfacial tension. For example review of published information on ATPS [14,15] shows that the difference between viscosities of two phases in the ATPS is more than 14 mPa s. Similarly, in conventional aqueous organic system, the difference in density is at least twice as that of ATPSs. In addition the interfacial tension is more than 13 mN m<sup>-1</sup> in aqueous organic two phase systems, whereas in the ATPS it is in the range of 10<sup>-4</sup> to 10<sup>-1</sup> mN m<sup>-1</sup>. In view of this, it was thought desirable to investigate the drop formation in ATPSs. Based on the available information of aqueous organic systems, an attempt was made to develop a model for drop formation in ATPSs and compare the predicted values with the experimental as well as the values predicted by the models reported in the literature.

\* Corresponding author. Tel.: +91-821-251-3910; fax: +91-821-251-7233.

E-mail address: [eng@cscftri.ren.nic.in](mailto:eng@cscftri.ren.nic.in) (K.S.M.S. Raghavarao).

<sup>1</sup> Present address: Mycolgy Laboratory, DAI, Wodsworth center, NYSDOH, Albany, NY 12208, USA.

## 2. Materials and methods

### 2.1. Materials

Polyethylene glycol ( $M_r$  6000) was procured from Sisco Research Labs., Bombay, India. Potassium dihydrogen phosphate and di-potassium hydrogen phosphate were procured from Ranbaxy Chemicals, Punjab, India.

### 2.2. Preparation of aqueous two phase systems

Predetermined, weighed quantities of polyethylene glycol and potassium phosphates (mono/di) were added to a known quantity of deionized water (Milli-Q, Millipore, Bedford, MA, USA), to make the total weight of the system to 100% on w/w basis. The mixture was mixed thoroughly for about an hour and allowed overnight to equilibrate. The equilibrated phases were separated and used for the study.

The physical properties of the phases were measured. Density was measured by specific gravity bottle and viscosity by Ostwald viscometer at constant temperature.

### 2.3. Experimental setup

The schematic diagram of the experimental setup is shown in Fig. 1a. A glass column of 95 cm height and 3.4 cm diameter was used to hold the continuous phase. The diameters of different capillaries were measured using a microscope Laborlux model of Leica, Germany. The height of the continuous phase was kept at a predetermined level. The dispersed phase was sparged through the capillary and flow rate was varied using a needle valve.

### 2.4. Experimental procedure

The drop formation was studied by employing both light (PEG rich) and heavy (salt rich) phases as the dispersed phase. The reservoir was first filled with the dispersed phase, then the continuous phase was added slowly into the column until a desired height was achieved. The flow of the dispersed phase from the reservoir was then started so as to form individual drops at the tip of the capillary. The flow rate was measured by noting the time for a definite volume change. The frequency of drop formation was adjusted in such a way that the drops fall/rise one after the other without coalescing. This ensured that the preceding drop did not influence the subsequent drop. The drop volume was estimated by measuring the number of drop ( $N$ ) at a particular time ( $T$ ) and noting the flow rate ( $Q$ ) (which was always kept less than  $Q_{jet}$ ). Thus, the experiential drop volume can be calculated as:

$$V = \frac{QT}{N} \quad (1)$$

## 3. Theoretical aspects

The models proposed in the literature for the prediction of the drop volume of aqueous organic systems are either based on force balance [10,16] or geometric treatments [9,17]. It is not surprising that, these models are successful only under restricted conditions, because of the complexity of the drop formation process. Further, drop volumes estimated using these models deviated considerably from the values in case of ATPSs.

### 3.1. At low flow rates

There are four major forces, which act on a drop during its formation at the tip of a capillary. The buoyancy and kinetic forces act to separate the drop from the capillary. The drag force and the interfacial tension exerted by the continuous phase act in opposite direction. At low flow rates, it was assumed that the drag and kinetic forces are very low and hence can be neglected. The buoyancy force is given by:

$$F_B = V_S \Delta \rho g \quad (2)$$

The interfacial tension force is given by:

$$F_\sigma = \pi D_n \gamma \quad (3)$$

At static condition, these forces are equal and opposite, hence the volume of the drop at this stage can be written as:

$$V_S = \frac{\pi D_n \gamma}{\Delta \rho g} \quad (4)$$

### 3.2. At high flow rates

At relatively higher flow rates, the kinetic and drag forces will come into picture where the kinetic force is given by:

$$F_K = \rho v_D Q \quad (5)$$

and according to Hadamard–Rybczynski, the drag force with internal circulation can be given as:

$$F_D = 4\pi r \mu_C v \left( \frac{\mu_C + \mu_D}{0.66\mu_C + \mu_D} \right) \quad (6)$$

Buoyancy and kinetic forces (lifting forces) pull the drop away from tip of the capillary, whereas interfacial tension and drag forces (restraining forces) try to keep the drop at capillary. At equilibrium condition, the restraining and lifting forces are equal and opposite.

$$F_B + F_K = F_\sigma + F_D \quad (7)$$

After substituting the appropriate expressions for the forces and rearranging Eq. (7), we get:

$$V_E = \frac{\pi D_n \gamma}{g \Delta \rho} + \frac{4\pi r \mu_C v}{g \Delta \rho} \left( \frac{\mu_C + \mu_D}{0.66\mu_C + \mu_D} \right) - \frac{\rho_D v_D Q}{g \Delta \rho} \quad (8)$$

which gives the volume of drop at the tip of capillary in equilibrium condition.

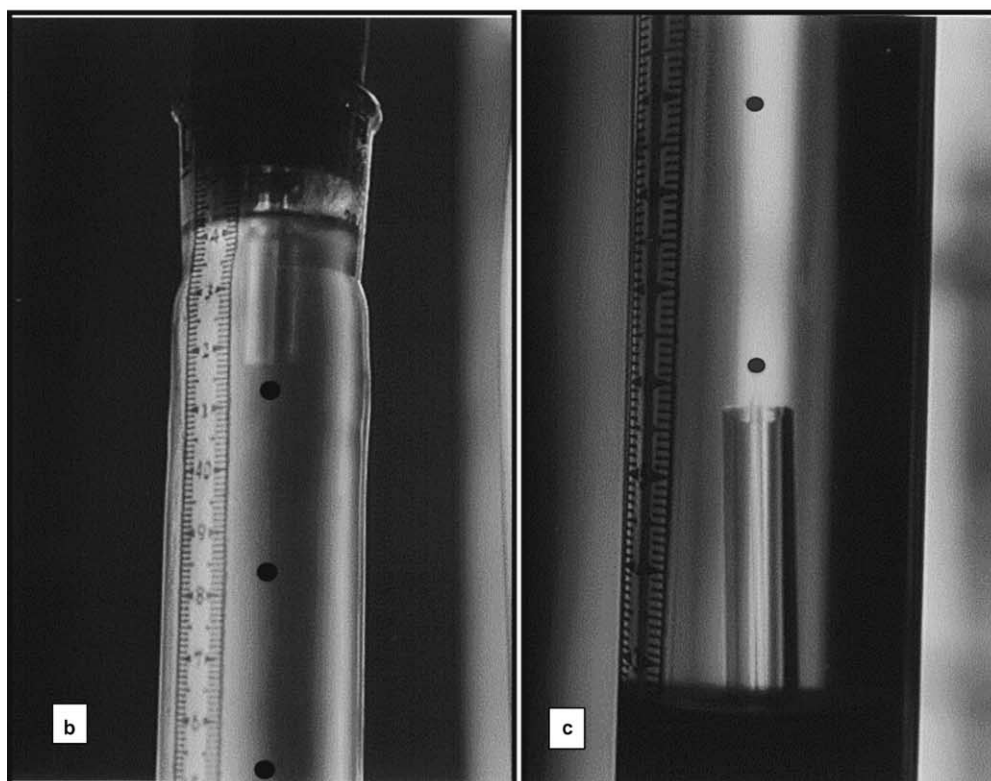
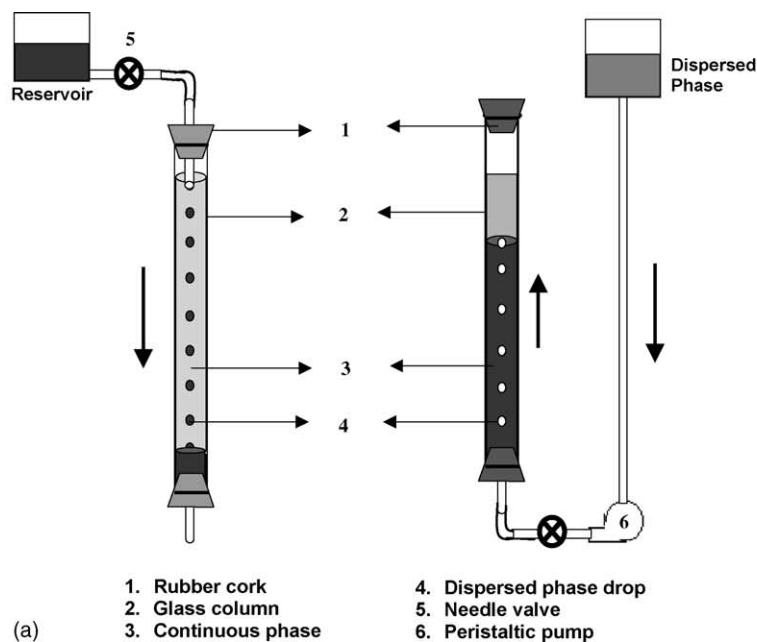


Fig. 1. (a) Experimental set up for drop dynamics studies; (b) heavy (salt rich) phase as a disperse phase; (c) light (PEG rich) phase as a disperse phase.

Before this detaches from the capillary a considerable amount of liquid flows into the drop ( $V_N$ ) and it starts growing further. Thus, expression for the final drop volume can be written as:

$$V_F = V_S + V_N \quad (9)$$

So, to obtain the final volume of the drop it is necessary to estimate this additional flow of liquid into the drop, which

can be calculated as:

$$V_N = Qt \quad (10)$$

where  $Q$  is volumetric flow rate through capillary and  $t$  is the time taken by the drops to detach during which additional liquid flows into it.

To evaluate this time  $t$  the force balance equation has to be solved and the various forces to be considered during the

drop detachment are Kinetic force, which is given by:

$$F_K = \rho v_C Q \quad (11)$$

Buoyancy force, which is given by:

$$F_B = V_N \Delta \rho g = \Delta \rho g Q t \quad (12)$$

and the drag force, which is given by:

$$F_D = 4\pi r \mu_C v_C \left( \frac{\mu_C + \mu_D}{0.66\mu_C + \mu_D} \right) \quad (13)$$

where  $v_C$  is the velocity of the dispersed phase inside the capillary.

The algebraic sum of these forces is equal to the rate of change of momentum of the drop:

$$\frac{dmv}{dt} = \Delta \rho g Q t + \rho v_C Q - 4\pi r \mu_C v_C \left( \frac{\mu_C + \mu_D}{0.66\mu_C + \mu_D} \right) \quad (14)$$

The interfacial tension in aqueous two phase system is very low and can be neglected during the drop detachment. And the mass of the drop 'm' can be assumed to be constant and equal to the mass of the static drop, as there is not much growth before detachment. Thus, the mass term can be given as:

$$m = V_S \rho_D + \frac{11}{16} V_S \rho_C \quad (15)$$

where  $11/16(V_S \rho_C)$  is the correction factor, which accounts for the inertia of the continuous phase. It assumes the flow around the drop is irrotational and unseparated as suggested by Davidson and Schuler [18].

Eq. (14) can be written as:

$$m \frac{dv}{dt} = \Delta \rho g Q t + \rho v_C Q - 4\pi r \mu_C v_C \left( \frac{\mu_C + \mu_D}{0.66\mu_C + \mu_D} \right) \quad (16)$$

The above equation is a first order linear differential equation, the solution of which is:

$$v = \frac{C}{A} + B \left( \frac{t}{A} - \frac{1}{A^2} \right) + \left( \frac{B}{A^2} - \frac{C}{A} \right) C \exp[-At] \quad (17)$$

where

$$A = \frac{4\pi r \mu_C}{m} \left( \frac{\mu_C + \mu_D}{0.66\mu_C + \mu_D} \right), \quad B = \frac{\Delta \rho g Q}{m},$$

$$C = \frac{Q v_C \rho_D}{m}$$

The velocity  $v_C$  of the dispersed phase inside the capillary is very low, hence  $C$  can be neglected. Then the Eq. (17) reduce to:

$$v = B \left( \frac{t}{A} - \frac{1}{A^2} \right) \quad (18)$$

The above equation can be utilized to explain the growth of the drop and that is written as:

$$v = \frac{dr}{dt} = \frac{Bt}{A} - \frac{B}{A^2} \quad (19)$$

where  $dr/dt$  is the growth in radius of drop with respect to time. On integration, the above equation becomes:

$$r = \frac{Bt^2}{2A} - \frac{Bt}{A^2} + K \quad (20)$$

Applying the boundary conditions to Eq. (20):

$$t = 0, \quad r = 0, \quad K = 0; \quad t = t, \quad r = xD_n$$

It was assumed that the radius of drop is equal to the  $x$  times the capillary diameter at time  $t$ , where  $x$  is the correction factor to account for the dependency of drop size on the capillary diameter (similar to the static drop size dependency on the capillary diameter). Photographic measurements (Fig. 1b and c) indicated that the drop diameter was about two times the capillary diameter employed in case of salt rich phase as the dispersed phase (that is  $x = 1.0$ ) and about 1.5 times in case of PEG rich phase as the dispersed phase (that is  $x = 0.75$ ).

Then the Eq. (20) becomes:

$$\frac{Bt^2}{2A} - \frac{Bt}{A^2} - xD_n = 0 \quad (21)$$

and

$$t = \frac{1}{A} + \left( \frac{1}{A^2} + \frac{2Ax D_n}{B} \right)^{1/2} \quad (22)$$

Then the final drop volume is obtained from Eqs. (9) and (10).

#### 4. Results and discussion

The drop volumes were evaluated as a function of flow rate for capillaries of different diameters and systems of different compositions. The diameter of the capillaries used in the study is shown in Table 1. The phase composition and physical properties of systems used are tabulated in Tables 2 and 3, respectively. The proposed model considers drop formation to take place in a single stage at low flow rates (Eq. (4)) and in two stages at high flow rates (Eq. (9)). Each case is discussed separately for light (PEG rich) and heavy (salt rich) phase as the disperse phase. Drop volumes were

Table 1  
Dimensions of the capillary

SI. no.	Capillary	Diameter of nozzle (m)
1	C <sub>1</sub>	$5.04 \times 10^{-4}$
2	C <sub>2</sub>	$9.24 \times 10^{-4}$
3	C <sub>3</sub>	$13.26 \times 10^{-4}$

Table 2  
Composition of the phase systems

System no.	Composition
1	12% PEG + 12.4% (8.26 di and 4.13 mono) potassium phosphate + 75.6% distilled water
2	7.93% PEG + 15.3% (10.2 di and 5.1 mono) potassium phosphate + 76.74% distilled water

Table 3  
Physical properties of systems at 25 °C

System no.	Densities (kg m <sup>-3</sup> )		Viscosity of phases (mPa s)		Interfacial tension (mN m <sup>-1</sup> )
	PEG	Salt	PEG	Salt	
1	1077	1159	16.72	1.55	0.545 <sup>a</sup>
2	1073	1147	14.32	1.60	0.360 <sup>a</sup>

<sup>a</sup> From literature [17].

predicted by the proposed model as well as the models reported in the literature, static model with Harkins and Brown correction factor at low flow rate [19] and two stage model of Rao et al., at high flow rate.

#### 4.1. Light (PEG rich) phase as a disperse phase

The variation in drop volume with respect to flow rate for the situation where PEG rich phase is dispersed into salt rich phase are shown in Figs. 2–4 and Table 4.

##### 4.1.1. At low flow rates

The reported flow regime for aqueous organic systems in which kinetic and drag force can be neglected during prediction of drop volume is of the order of  $10^{-10}$  m<sup>3</sup> s<sup>-1</sup>

[19]. The corresponding flow rate in case of ATPSs is  $(7 \text{ to } 12) \times 10^{-10}$  m<sup>3</sup> s<sup>-1</sup>.

Fig. 2 and Table 4 show that the drop volume predicted by the proposed single stage model (Eq. (4)) matches with the experimental drop volume more closely than the static model with Harkins and Brown correction factor (H & B correction factor) reported in the literature for conventional aqueous organic systems. From this figure and table, it can also be observed that the drop volumes obtained by the latter model were too low as compared to the experimental values. This could probably be reasoned as follows. H & B correction factor accounts for the fraction of drop at the tip of the capillary after drop detaches and the fraction will be high when interfacial tension value is high ( $(20 \text{ to } 50) \times 10^{-3}$  N m<sup>-1</sup>) as in the case of aqueous–organic system. But in case of ATPSs, interfacial tension values are very low and for the systems studied are  $0.36 \times 10^{-3}$  and  $0.545 \times 10^{-3}$  N m<sup>-1</sup>. In view of low magnitude of interfacial forces, this correction factor under predicts the drop volume.

##### 4.1.2. At high flow rates

It may be noted that, the flow regime for two stage drop formation in case of aqueous–organic systems inferred from literature is of order of  $10^{-8}$  to  $10^{-7}$  m<sup>3</sup> s<sup>-1</sup> [10]. The corresponding flow regime in ATPSs is of the order of  $10^{-9}$  m<sup>3</sup> s<sup>-1</sup>, which is lower by at least one order of magnitude than that of aqueous–organic systems.

Figs. 3 and 4 show experimental and predicted drop volumes at different flow rates by the proposed two-stage model (Eq. (9)) and that of Rao et al. [10]. Although both the models are based on two stage drop formation, former is developed for ATPSs while latter for aqueous–organic systems. The close matching of the drop volumes predicted by these two stage models with the experimental values in the

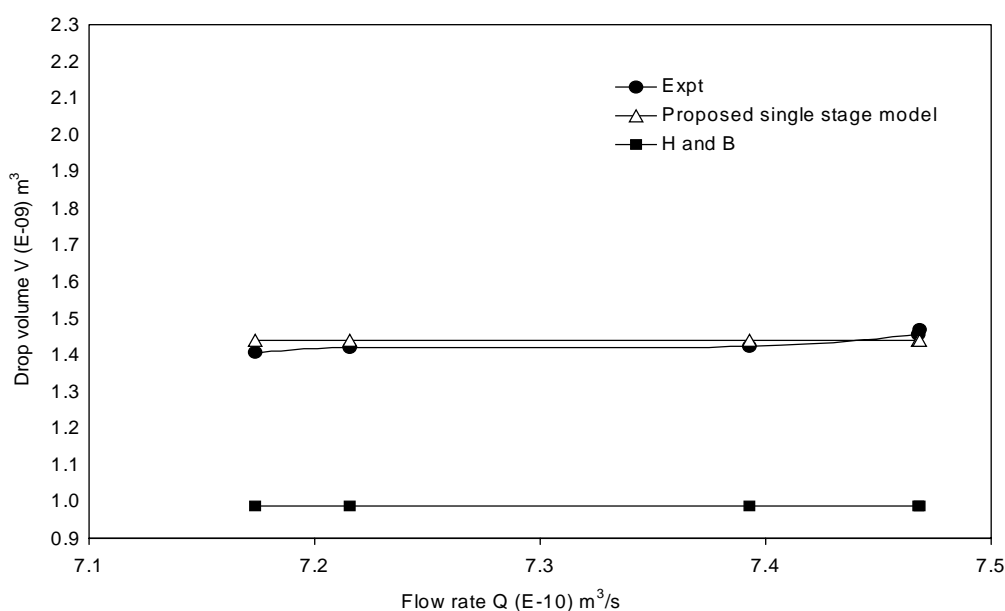


Fig. 2. Volume of drop formation at various flow rates (system 2, PEG sparg C<sub>2</sub>).

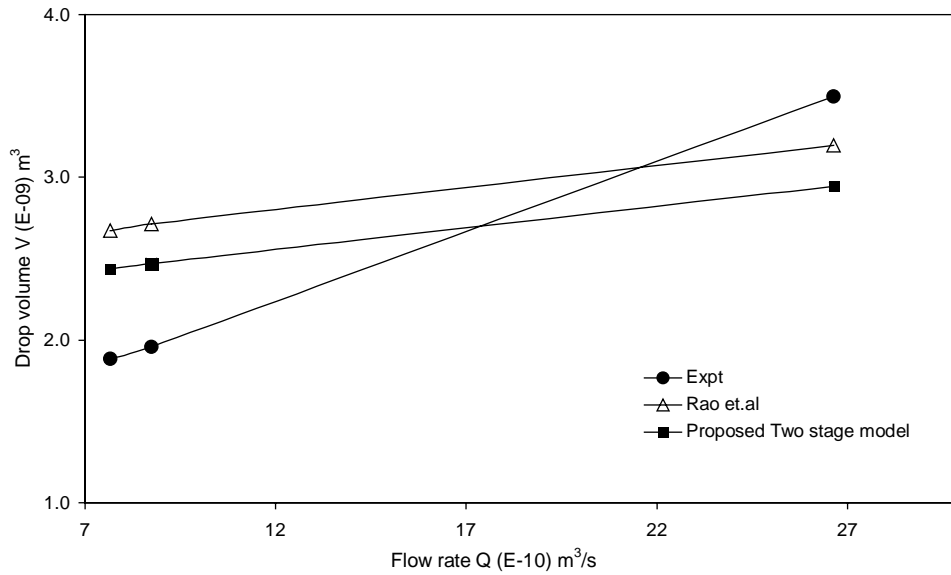
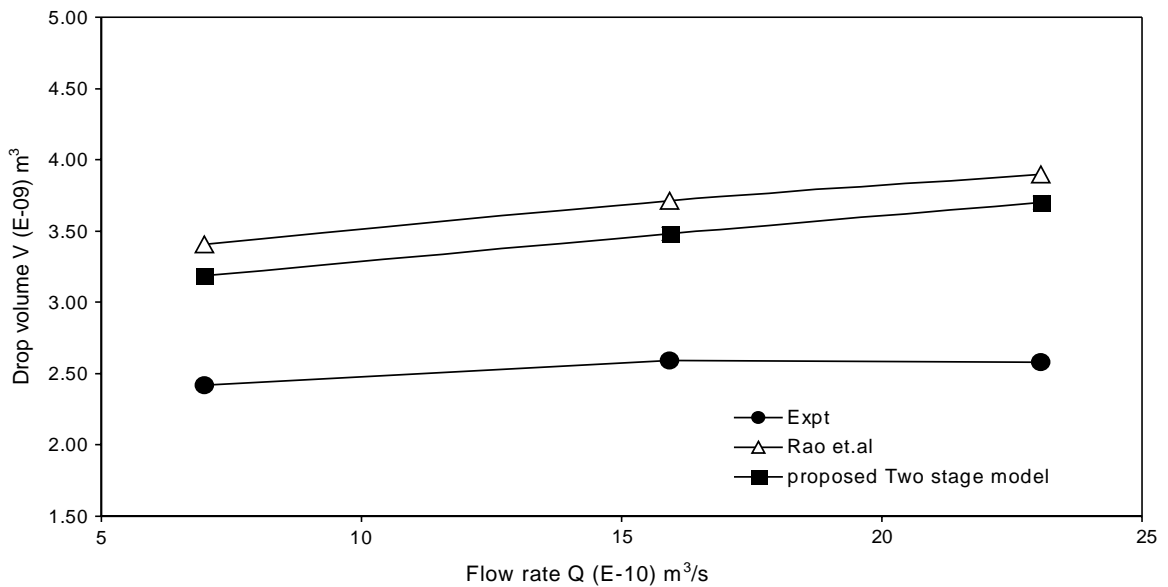
Fig. 3. Volume of drop formation at various flow rates (system 2, PEG sparg C<sub>3</sub>).Fig. 4. Volume of drop formation at various flow rates (system 1, PEG sparg C<sub>3</sub>).

Table 4

Comparison of experimental drop volumes with the proposed and literature values at various low flow rates

SI. no.	Flow rate ( $\times 10^{-10}$ , $\text{m}^3 \text{s}^{-1}$ )	Experimental ( $\times 10^{-9}$ , $\text{m}^3$ )	Proposed (Eq. (4)) ( $\times 10^{-9}$ , $\text{m}^3$ )	H & B ( $\times 10^{-9}$ , $\text{m}^3$ )	System	Mode of sparging	Capillary
1	6.73	0.90	0.79	0.59	2	PEG	C1
2	7.19	1.09	1.07	0.81	1	PEG	C1
3	9.86	1.63	1.96	1.38	1	PEG	C2
4	9.18	2.41	1.96 <sup>a</sup>	1.38 <sup>b</sup>	1	Salt	C2

Note: The reported values are the average of four values.

<sup>a</sup> Eq. (9).

<sup>b</sup> Rao et al. [10].

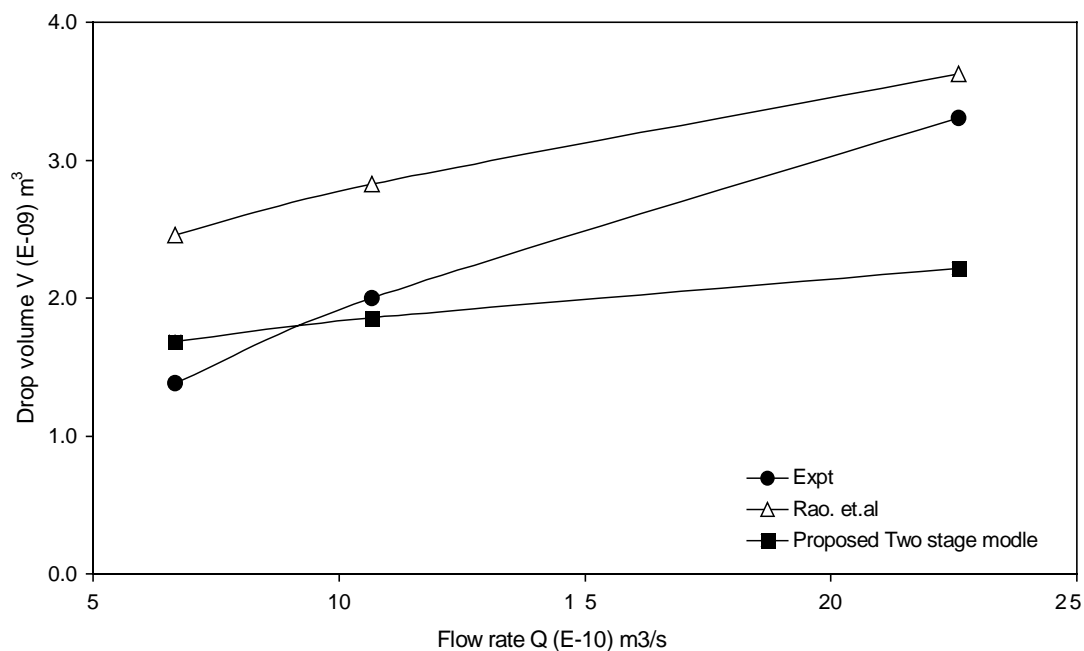


Fig. 5. Volume of drop formation at various flow rates (system 1, salt sparg C<sub>1</sub>).

present study indicate that the kinetic and drag forces cannot be ignored in this flow regime. Furthermore, from these figures, it can be observed that the drop volumes predicted by proposed model match with the experimental drop volume more closely than that of Rao et al. (especially in the flow range of  $(12 \text{ to } 20) \times 10^{-10} \text{ m}^3 \text{ s}^{-1}$ ). This is mainly due to the more accurate estimation of the drag forces in the proposed model by accounting the internal circulation of the droplets.

#### 4.2. Heavy (salt rich) phase as a disperse phase

The effects of flow rates on drop volumes, when a salt rich phase is dispersed in the PEG rich phase are shown in Figs. 5–7 and, Tables 4 and 5.

##### 4.2.1. At low flow rates

The flow regime was observed to be almost same for both sparging modes where kinetic and drag forces could be

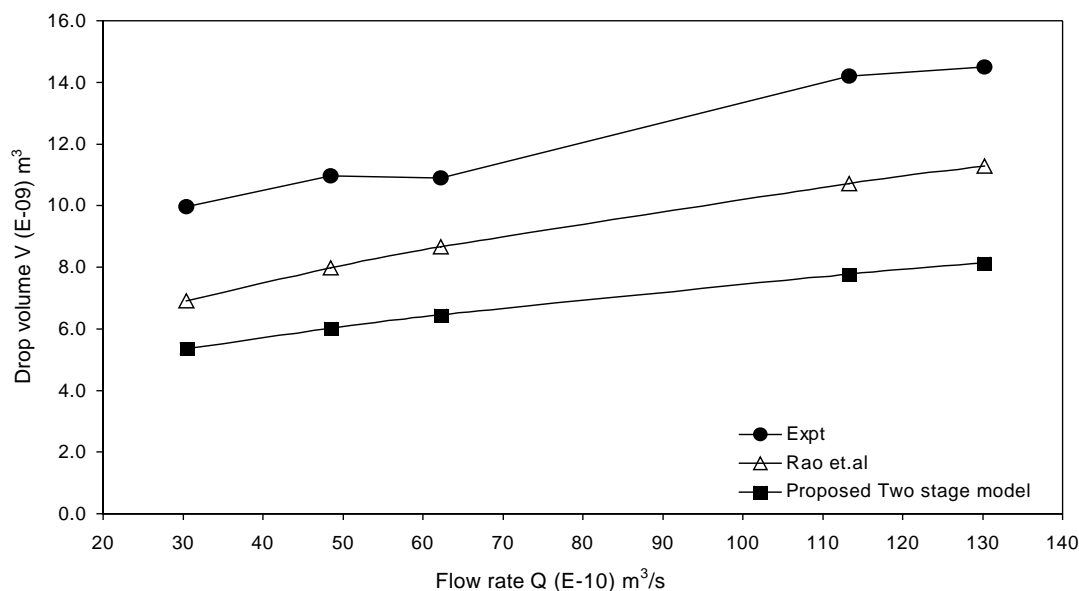


Fig. 6. Volume of drop formation at various flow rates (system 1, salt sparg C<sub>3</sub>).

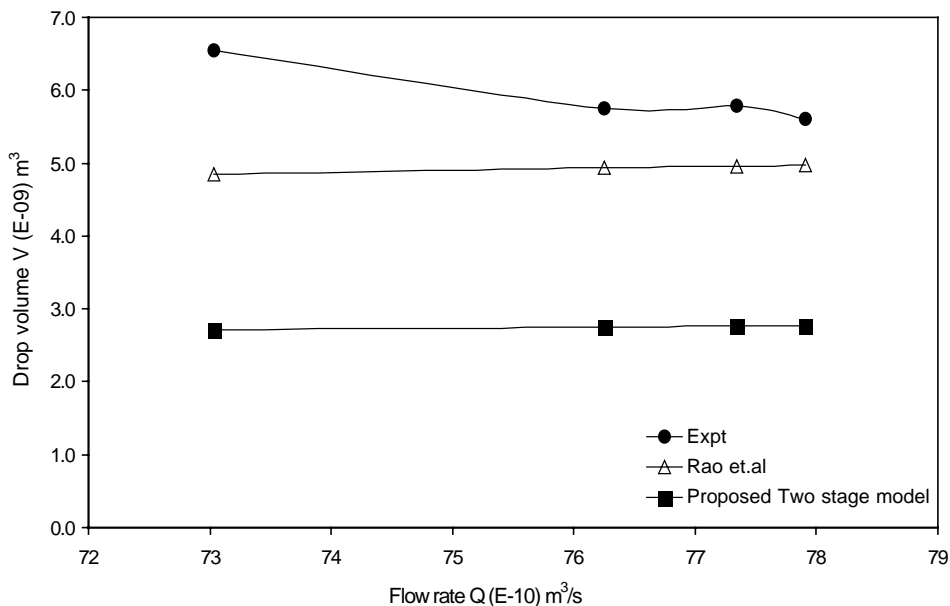


Fig. 7. Volume of drop formation at various flow rates (system 2, salt sparg  $C_1$ ).

neglected during prediction of drop volumes (Table 4). Similarly, as discussed previously in PEG rich phase as disperse phase, the growth of the drop is expected to be essentially radial in this case as well.

Table 4 shows that the drop volumes predicted by proposed single stage model (Eq. (4)) matches with the experimental values more closely than reported model (static model with H & B correction factor [19]). This could be due to the similar reason as discussed in case of light (PEG rich) phase as the disperse phase. Furthermore, from this Table, it can also be inferred that the extent of under prediction of drop volume by the reported model was relatively much higher when heavy (salt rich) phase formed the disperse phase (Table 4) compared to the situation where light (PEG rich) phase formed the disperse phase (Fig. 2). This is due to the fact that the fraction of the drop associated at tip of the capillary in the direction of gravity will be less than

that of opposite to gravity. It can also be noted that the observed drop volume in this mode of sparging is higher when compared to the situation where PEG rich phase is sparged. This is mainly due to higher viscosity of continuous phase, which prolongs the drop formation time.

#### 4.2.2. At high flow rates

The flow regimes for two stage drop formation in case of systems 1 and 2 are  $(8 \text{ to } 20) \times 10^{-10}$ , and  $(20 \text{ to } 70) \times 10^{-10} \text{ m}^3 \text{ s}^{-1}$ , respectively. The growth of the drop in this flow regime is expected to take place similarly as mentioned previously for sparging of light (PEG rich) phase at high flow rates.

Fig. 5 and Table 5 show the effect of flow rate on experimental and predicted drop volumes (by proposed two-stage model (Eq. (9))) and reported model of Rao et al. [10]. From above figure and table, it can be observed that the

Table 5

Comparison of experimental drop volumes with the proposed and literature values at various high flow rates

SI. no.	Flow rate ( $\times 10^{-10}$ , $\text{m}^3 \text{ s}^{-1}$ )	Experimental ( $\times 10^{-9}$ , $\text{m}^3$ )	Proposed (Eq. (9)) ( $\times 10^{-9}$ , $\text{m}^3$ )	Rao et al. [10] ( $\times 10^{-9}$ , $\text{m}^3$ )
<i>System 2, salt sparg, <math>C_2</math></i>				
1	39.67	4.09	3.56	5.10
2	61.79	4.94	4.09	6.01
3	72.22	5.36	4.31	6.38
<i>System 2, salt sparg, <math>C_3</math></i>				
4	14.25	2.14	3.61	4.54
5	25.32	3.53	4.23	5.49
6	30.70	3.84	4.43	5.70
7	45.23	4.07	4.94	6.47
8	59.30	4.74	5.37	7.11
9	75.77	5.95	5.80	7.78

drop volume predicted by proposed model matches with the experimental drop volume more closely than the reported model. Further, at high flow rates the drop volumes is higher than that of the mode where PEG rich phase formed the disperse phase and the difference is more prominent when compared to that at low flow rates. This could be explained as follows. When, the droplets of salt rich phase (of low viscosity) sparged through PEG rich phase (of high viscosity), drag experienced by drop is nearly 15 to 20 times more than that of PEG rich phase droplets sparged through salt rich phase. This high magnitude of drag is expected to increase the drop formation time by allowing drop to stay at the tip of the capillary for longer duration thereby, resulting in bigger drop size for a given flow rate (Fig. 6). Furthermore, higher drag force tends to increase not only the internal circulation within the droplet but also to change the shape of the drop from spherical shape, which was also observed visually.

At still higher flow rates, neither the proposed nor reported models could predict the drop volumes satisfactory (Figs. 6 and 7). In this flow regime, drop formation mechanism is substantially governed by unidirectional flow arising from capillary and significant difference is expected in kinetic force due to synergetic effect of gravity and parabolic distribution of velocity component within the capillary that limits performance of two-stage models.

## 5. Conclusions

The flow regime where force balance analysis could be employed to predict drop volumes in case of ATPSS varies from  $(1.6 \text{ to } 75) \times 10^{-10} \text{ m}^3 \text{ s}^{-1}$  depending upon the diameter of capillary, phase system and mode of drop formation. At low flow rates, single stage drop formation model (Eq. (4)) as such can be adopted for prediction of drop volume. However, at high flow rates, kinetic and drag forces has to be accounted in force balance analysis and it is more appropriate to consider the internal circulation in the droplet while estimating drag force. At these flow rates, two-stage drop formation model (Eq. (9)) can be used to predict the drop volume, where the additional volume of disperse phase enters to the drop during its detachment has to be accounted. The proposed models explain both the drop formation modes in ATPSS and able to predict the drop volume during its formation from the tip of capillary.

## 6. Nomenclature

$D_n$	diameter of capillary (m)
$D_S$	static diameter of drop (m)
$F_B$	buoyancy force ( $\text{kg m s}^{-2}$ )
$F_D$	drag force ( $\text{kg m s}^{-2}$ )

$F_K$	kinetic force ( $\text{kg m s}^{-2}$ )
$F_\sigma$	interfacial tension force ( $\text{kg m s}^{-2}$ )
$g$	acceleration due to gravity ( $\text{m s}^{-2}$ )
$m$	mass of drop (kg)
$Q$	volumetric flow rate of disperse phase ( $\text{m}^3 \text{ s}^{-1}$ )
$r$	radius of growing drop (m)
$t$	break time factor for drop (s)
$v$	velocity (growth) of the drop ( $\text{m s}^{-1}$ )
$v_C$	velocity of disperse phase inside the capillary ( $\text{m s}^{-1}$ )
$v_D$	velocity of disperse drop ( $\text{m s}^{-1}$ )
$V_F$	final volume of drop ( $\text{m}^3$ )
$V_N$	additional volume enters to drop during breakage ( $\text{m}^3$ )
$V_S$	static volume of drop ( $\text{m}^3$ )
$x$	correction factor defined in Eq. (21)

### Greek letters

$\gamma$	interfacial tension ( $\text{N m}^{-1}$ )
$\mu_C$	viscosity of continuous phase (mPa s)
$\mu_D$	Viscosity of disperse phase (mPa s)
$\Delta\rho$	density difference between two phase ( $\text{kg m}^{-3}$ )
$\rho_C$	density of continuous phase ( $\text{kg m}^{-3}$ )
$\rho_D$	density of disperse phase ( $\text{kg m}^{-3}$ )

## Acknowledgements

The authors wish to thank Dr. V. Prakash, Director, CFTRI, for his keen interest in extractions using ATPSS. One of the authors (RSB) gratefully acknowledges CSIR, India for the award of a Senior Research Fellowship.

## References

- [1] P.A. Albertsson, Partitioning of Cell Particles and Macromolecules, third ed., Wiley, New York, 1986.
- [2] H. Walter, D.E. Brooks, D. Fisher (Eds.), Partitioning in Aqueous Two Phase Systems: Theory, Methods, Uses and Applications to Biotechnology, Academic Press, Orlando, FL, 1985.
- [3] B.Y. Zaslavsky, Aqueous Two Phase Partitioning: Physical Chemistry and Bioanalytical applications, Marcel Dekker, New York, 1995.
- [4] K.S.M.S. Raghavarao, N.K. Rastogi, M.K. Gawthaman, N.G. Karanth, Adv. Appl. Microbiol. 41 (1995) 97.
- [5] K.S.M.S. Raghavarao, M.R. Guinn, P. Todd, Sep. Purif. Methods 27 (1998) 1.
- [6] J.B. Joshi, K.S.M.S. Raghavarao, S.B. Sawant, K.M. Rostani, S.K. Sikdar, Bioseparations 1 (1990) 358.
- [7] S.B. Sawant, J.B. Joshi, S.K. Sikdar, Biotech. Bioeng. 36 (1990) 109.
- [8] C.B. Haywarth, R.E. Treybol, Ind. Eng. Chem. 41 (1950) 1174.
- [9] H.R. Null, H.F. Johnson, AIChE. J. 4 (1958) 273.
- [10] E.V.L.N. Rao, R. Kumar, N.R. Kuloor, Chem. Eng. Sci. 21 (1966) 867.
- [11] G.F. Scheele, O.B. Meister, AIChE. J. 14 (1968) 9.
- [12] R.Z. Tudose, S. Carstea Hung, J. Ind. Chem. 22 (1994) 15.

- [13] C.T. Chen, J.R. Maa, Y.M. Yang, C.H. Chang, *Int. Comm. Heat Mass Trans.* 28 (2001) 681.
- [14] C. Prafulla, M. Bhawsar, A.B. Pandit, S.B. Sawant, J.B. Joshi, *Chem. Eng. J.* 55 (1994) B1.
- [15] P.M. Bhavasar, K.R. Jafarabad, A.B. Pandit, S.B. Sawant, J.B. Joshi, *Can. J. Chem. Eng.* 74 (1996) 852.
- [16] L.E.M. De Chazal, J.T. Ryan, *AICHE J.* 17 (1971) 1226.
- [17] K.R. Jafarabad, S.B. Sawant, J.B. Joshi, S.K. Sikdar, *Chem. Eng. Sci.* 47 (1992) 57.
- [18] J.F. Davidson, B.O.G. Schuler, *Trans. Inst. Chem. Eng.* 38 (1960) 144.
- [19] W.D. Harkins, F.E. Brown, *J. Am. Chem. Soc.* 41 (1919) 499.